



HAL
open science

Effects of hygrothermal aging on chemical, physical, and mechanical properties of poly(3-hydroxybutyrate-co-3-hydroxyvalerate)/Cloisite 30B bionanocomposite

Kahina Iggui, Mustapha Kaci, Nicolas Le Moigne, Anne Bergeret

► To cite this version:

Kahina Iggui, Mustapha Kaci, Nicolas Le Moigne, Anne Bergeret. Effects of hygrothermal aging on chemical, physical, and mechanical properties of poly(3-hydroxybutyrate-co-3-hydroxyvalerate)/Cloisite 30B bionanocomposite. *Polymer Composites*, 2021, 42 (4), p.1878-1890. 10.1002/pc.25943 . hal-03113919

HAL Id: hal-03113919

<https://imt-mines-ales.hal.science/hal-03113919>

Submitted on 25 Jan 2021

HAL is a multi-disciplinary open access archive for the deposit and dissemination of scientific research documents, whether they are published or not. The documents may come from teaching and research institutions in France or abroad, or from public or private research centers.

L'archive ouverte pluridisciplinaire **HAL**, est destinée au dépôt et à la diffusion de documents scientifiques de niveau recherche, publiés ou non, émanant des établissements d'enseignement et de recherche français ou étrangers, des laboratoires publics ou privés.

Effects of hygrothermal aging on chemical, physical, and mechanical properties of poly(3-hydroxybutyrate-co-3-hydroxyvalerate)/Cloisite 30B bionanocomposite

Kahina Iggui^{1,2,3} | Mustapha Kaci¹ | Nicolas Le Moigne³ | Anne Bergeret³

¹Laboratoire des Matériaux Polymères Avancés (LMPA), Université de Bejaia, Bejaia, Algeria

²Institut de Technologie, Université Akli Mohand Oulhadj, Bouira, Algeria

³Polymers Composites and Hybrids (PCH), IMT-Mines Ales, Ales, France

Correspondence

Kahina Iggui, Laboratoire des Matériaux Polymères Avancés (LMPA), Université de Bejaia, 06000, Algeria.

Email: iguikahina@yahoo.fr

Abstract

Hygrothermal aging of neat poly(3-hydroxybutyrate-co-3-hydroxyvalerate) (PHBV) and PHBV filled with an organomodified montmorillonite (C30B) at 3wt. was investigated at 65°C and 100% relative humidity (RH) up to 100 days. FT-IR data indicated that the carbonyl intensity index decreased with exposure time for both samples, while the main degradation mechanism occurred through hydrolysis reaction. This led to chain scissions resulting in a decrease in molar mass. Water absorption increased with exposure time for both neat PHBV and PHBV/C30B (3wt%) bionanocomposite. Differential scanning calorimetry measurements showed a decrease in both crystallinity index and melting temperature after hygrothermal aging and thermogravimetric analysis data indicated also a decrease in thermal stability. Mechanical and viscoelastic properties were also altered, being, however, more pronounced for the neat PHBV. Overall, the PHBV bionanocomposite exhibited a better resistance toward hygrothermal aging at 65°C and 100% RH.

KEYWORDS

bionanocomposite, chain scission, crystallinity, dynamic mechanical properties, hygrothermal aging, PHBV, thermal stability

1 | INTRODUCTION

Poly(3-hydroxybutyrate-co-3-hydroxyvalerate) (PHBV) is an aliphatic biopolyester of the polyhydroxyalkanoates (PHAs) family produced from a variety of bacteria^[1-2]. Due to its biodegradability, biocompatibility and interesting physical properties, PHBV is an answer to nowadays-environmental issues and emerges in consumer markets, especially in food packaging and biomedical applications^[3-4]. However, PHBV has limited mechanical and thermal properties, which restricts its use in other industrial fields^[5].

To overcome these drawbacks, the incorporation and dispersion of organomodified montmorillonite (OMMT) such as Cloisite 30B in PHBV could be an effective method to produce bionanocomposite materials with enhanced functional properties^[6-8]. However, when exposed to environmental factors, such as temperature, humidity, UV light etc., PHBV undergoes aging and degradation^[9-10]. In this regard, hygrothermal aging combines the effects of both humidity and temperature, which often result in irreversible changes in the chemical structure, molar mass and physical properties of the polymer materials^[11-12]. According to the literature^[13-15], in hygrothermal aging, polyesters undergo an auto-catalytic random chain scission and ester bond hydrolysis is the main degradation mechanism^[16-18]. The hydrolysis

process can be sensitive to humidity, temperature, and environmental pressure^[19–20]. Generally, it is accelerated by the synergic effect of temperature and high humidity content^[21].

Several studies dealt with the hygrothermal behavior of different PHAs, mainly involving their blends and biocomposites reinforced with (ligno)-cellulosic fibers. In this topic, Zhuikov et al.^[22] studied the hydrolytic degradation of biopolyester poly-3-hydroxybutyrate (PHB) films with different molecular weights and different content ratios of 3-hydroxyvalerate(3-HV) with and without polyethylene glycol (PEG) used as the compatibilizer. The degradation of PHAs films was carried out in saline solution of phosphate-buffered saline (PBS) at 37°C and pH of 7.4 for 187 days. The authors reported that the total mass of (PHB-3HV) copolymer films with high-molecular weight and 17.6% and 9% of 3-hydroxyvalerate slightly decreased up to 8%–9%. Conversely, no significant changes were observed for the other samples even after 180 days. Hydrophobic character of all samples decreased after hydrolytic degradation, with a decrease in water contact angle by almost 17%. More recently, Mazur and Kuciel^[23] in their study on PHBV and wood fibers biocomposites filled at 7.5 and 15wt% exposed to hydrothermal aging in saline solution at 40°C, showed that the water absorption rate increased logically with fiber content ratio; the highest rate was observed for the biocomposite filled at 15wt%. After 2 weeks of aging, the tensile strength decreased slightly by almost 10% for the PHBV/wood fibers (15wt%) compared with that of the unexposed sample. Marinho et al.^[24] studied the effect of water absorption on the performance of PHB/babassu fibers biocomposites loaded at different filler content ratios, that is, 5, 10, and 20wt%. The authors concluded that the absorption process became slower as the fiber content increased. Water diffusion coefficient of PHB/babassu composite (20wt%) was about $4 \times 10^{-8} \text{ cm}^2 \text{ s}^{-1}$. The elastic modulus calculated at saturation decreased by 10%–30% with respect to fiber content, but tensile strength and elongation at break remained almost unchanged. Badia et al.^[25] studied the hydrothermal stability of PHBV/sisal fibers biocomposites at three temperatures 26, 36, and 46°C. The authors noticed that the effect of both temperature and percentage of fibers induced an increase of water diffusion rate. However, the water uptake was only affected by the fiber content. Also the mechanical properties of the biocomposites were altered; because the swelling of fibers induced cracks within the polymer as well as interfacial decohesion with the fibers. Ventura et al.^[26] also reported that moisture uptake can induce microcracks at the fiber-matrix interface with matrix damage and interfacial decohesion in PHB biocomposites reinforced with flax fibers. On the other hand,

the incorporation of clays can affect the inherent hydrophilicity of polyesters which in turn has an effect on the whole degradation mechanism. Silva et al.^[27] investigated hydrolytic degradation of PHB, PEG, and organophilic vermiculite (VMT) clay bionanocomposites (PHB/PEG/VMT) at 95/5/3wt% in saline solution at 37°C and pH = 7.4. They observed that the addition of the VMT clay led to a mass loss of about 5% in the fourth week of hydrolytic degradation and decreased the crystallinity. FT-IR results indicated that the occurrence of degradation process of pure PHB in the amorphous phases and was accelerated by the addition of reinforcement and compatibilizer agent, leading to increase of carbonyl index. Studies on degradation of PHBV/clays bionanocomposites under hygrothermal conditions have not been sufficiently addressed in the open literature. Therefore, further investigations are necessary to better understanding the effect of organo-modified montmorillonite on hydrolytic degradation of PHBV and its physical properties so as to better predict the material service life.

In this regard, the objective of the present work was to study the effect of hygrothermal aging on the chemical structure, the physical and the mechanical properties of neat PHBV and PHBV/OMMT bionanocomposite (3wt%) at 65°C and 100% HR in autoclave. Structural changes were investigated by FT-IR spectroscopy and size-exclusion chromatography (SEC) analysis. Thermal properties were determined by differential scanning calorimetry (DSC), while thermal stability was evaluated by thermogravimetric analysis (TGA). Tensile properties and viscoelastic properties were also determined. The morphological defects due to hygrothermal degradation were characterized by scanning electron microscopy (SEM) observations.

2 | EXPERIMENTAL METHODS

2.1 | Materials used and sample preparation

PHBV (PHI 002[®]) was commercialized by Nature Plast (France). The commercial organomodified Cloisite 30B (C30B) was purchased from Southern Clay Products, Inc. (USA).

PHBV and nanobiocomposite films samples of 500 μm thickness, named Cast PHBV and C-PHBV/3C30B (3wt%), respectively, were melt blended using a single-screw cast extruder by masterbatch dilution with neat PHBV of a PHBV/C30B mixture prepared by twin-screw extrusion. The preparation method of the masterbatch and films has been previously detailed in recent paper^[28]. ISO $\frac{1}{2}$ dumbbell specimens were cut from PHBV and bionanocomposite films.

2.2 | Hygrothermal aging

Hygrothermal aging has been recorded in a stainless steel autoclave (SANOCLAV) at atmospheric pressure, 100% RH and 65°C up to 100 days^[29]. Films of Cast PHBV and PHBV/3C30B bionanocomposite samples were vertically positioned above the distilled water surface. Aged specimens were collected periodically and dried in a vacuum oven at 60°C for 24 h. Finally the specimens were stored in vacuum chamber at ambient temperature and 2% RH for the subsequent chemical, physical, and mechanical characterizations.

2.3 | Characterization methods

2.3.1 | Water absorption

Weight gains of Cast-dried PHBV and dried C-PHBV/3C30B at 60°C in a vacuum oven during 24 h were measured by a gravimetric method. This method consists of removing at regular intervals the samples from an autoclave and weighing them with digital analytical balance. Five samples of each material were periodically removed from water, wiped and weighed. The weight gain $M(t)$ as a result of water absorption, was determined according to Equation (1):

$$M(t) = \frac{W(t) - Wd}{Wd} \quad (1)$$

where Wd and $W(t)$ correspond, respectively, to the weight of sample (the initial weight of dried sample before exposure to water absorption) and to the weight of the sample after a time t of exposure to water absorption. The water diffusion coefficient D was determined according to Fick's law and using Equation (2) adapted for long-time approximation^[30], that is, $0.4 < \frac{M(t)}{M_\infty} < 1$:

$$\frac{M(t)}{M_\infty} = 1 - \frac{8}{\pi^2} \exp\left(\frac{-D\pi^2 t}{e^2}\right) \quad (2)$$

where M_∞ is the weight gain at infinite time and e is half of the sample thickness, that is, 250 μm , because diffusion takes place from both sides.

2.3.2 | Size-exclusion chromatography (SEC)

SEC analysis was carried out by an Omni-SECT 60A system equipped with a Waters 410 differential refractometer. SEC analysis was conducted on neat PHBV,

Cast PHBV, and C-PHBV/3C30B bionanocomposite in a PL Gel 5-mm Mixed-C column (1 \times 600 mm). The chloroform was used as an eluent with a flow rate of 1 ml min⁻¹. Before injection, approximately 20 mg of each material were dissolved in 2 ml of chloroform over 1 h at 60°C. To remove any insoluble fractions or nanofiller, the solutions were filtered through a Phenex PTFE 0.2 mm filter. For calibration polystyrene standards were used. The average results of two tests of each sample were reported.

2.3.3 | Solubility test

In order to check whether there is the formation of gel fraction during hydrothermal aging, solubility tests were conducted by a Soxhlet apparatus. One gram of exposed and unexposed Cast PHBV and C-PHBV/3C30B bionanocomposite dried samples were dissolved in 100 ml of chloroform at 60°C for 1 h^[31].

2.3.4 | Fourier transform infrared spectroscopy (FT-IR)

FT-IR spectra of Cast PHBV and C-PHBV/3C30B bionanocomposite dried samples were performed on a BRUKER Vertex 70 spectrometer. The attenuated total reflectance (ATR) measurements were recorded for each material at a resolution of 4 cm⁻¹ and 32 scans from 4000–400 cm⁻¹.

2.3.5 | Differential scanning calorimetry (DSC)

A DSC analysis was carried out by a Pyris Diamond DSC thermal analysis system (PerkinElmer) using nitrogen as inert gas. Dried samples (15–20 mg) were sealed into aluminum pans and heating–cooling–heating was carried out in the temperature range starting from 30 to 200°C at a heating rate of 10°C min⁻¹. The crystallinity index (X_c) was calculated using Equation (3):

$$X_c = \frac{\Delta H_m}{W \cdot \Delta H_m^0} \times 100 \quad (3)$$

where ΔH_m (J.g⁻¹) is the melting enthalpy, ΔH_m^0 is the melting enthalpy of 100% crystalline PHBV ($\Delta H_m^0 = 146 \text{ J.g}^{-1}$ ^[32]) and W is the weight fraction of PHBV in the bionanocomposite sample. Three replicates were tested for each sample.

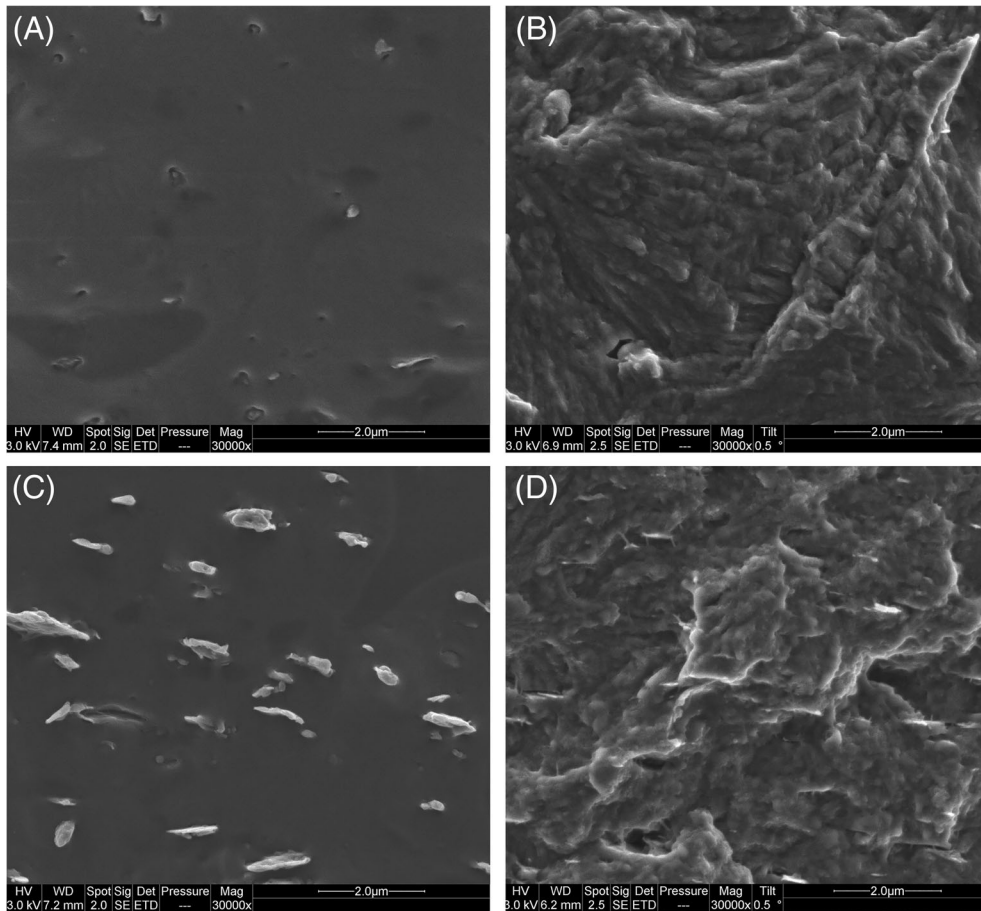


FIGURE 1 SEM images of fractured surface of Cast PHBV (A) before exposure (B) after 100 days of exposure and C-PHBV/3C30B bionanocomposite (C) before exposure and (D) after 100 days of exposure. SEM, scanning electron microscopy; PHBV, poly(3-hydroxybutyrate-co-3-hydroxyvalerate)

Samples	Exposure time (days)	\bar{M}_w ($\frac{g}{mol}$)	\bar{M}_n ($\frac{g}{mol}$)	\bar{D}
Neat PHBV	/	375,835	121,747	3.09
Cast PHBV	0	290,860	112,950	2.6
	30	105,299	46,680	2.3
	100	46,380	21,886	2.1
C-PHBV/3C30B	0	305,510	94,640	3.2
	30	138,603	64,573	2.2
	100	51,768	23,995	2.1

TABLE 1 Values of \bar{M}_w , \bar{M}_n and \bar{D} of neat PHBV, Cast PHBV, and C-PHBV/3C30B bionanocomposite as function of exposure time

Abbreviation: PHBV, poly(3-hydroxybutyrate-co-3-hydroxyvalerate).

2.3.6 | Thermogravimetric analysis (TGA-DTG)

Thermal stability of aged samples was evaluated by thermogravimetric analysis under nitrogen atmosphere. TGA-DTG thermograms were recorded with a Pyris Diamond thermogravimetric analyzer (PerkinElmer). Dried samples of an average weight of 10–12 mg were heated from 30 to 700°C, at a heating rate of 10 °C min⁻¹. Three replicates were tested for each sample.

2.3.7 | Dynamic mechanical analysis

The viscoelastic properties of aged samples were determined by DMA 50 dynamic mechanical analyzer (Metravib O3dB, France), under standard ISO 6721-10. The rectangular samples with a dimension of 35 × 5 × 0.5 mm were subjected to deformation in shear mode at 5 µm of amplitude and 5 Hz, in temperature range from -20 to 120°C at a heating rate of 3 °C min⁻¹.

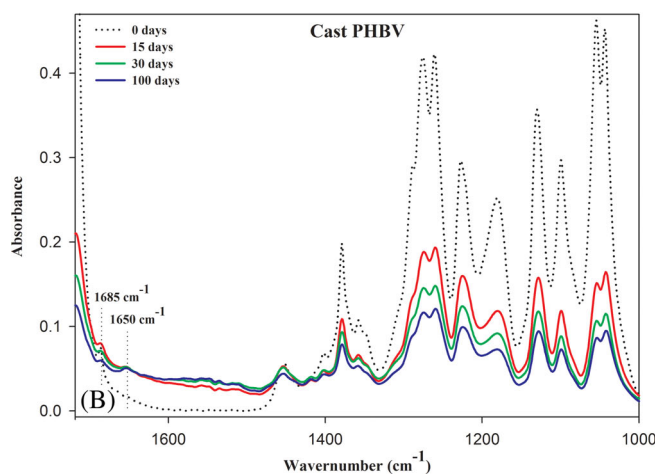
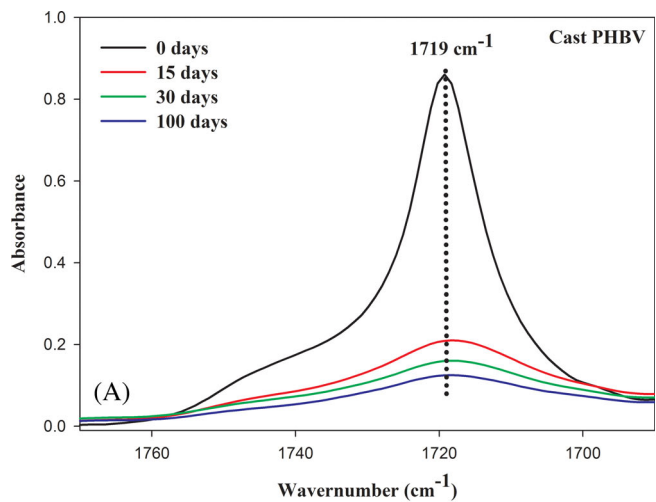


FIGURE 2 FT-IR spectra of Cast PHBV before and after exposure to hydrothermal aging recorded in the carbonyl region: (A) 1760–1700 cm^{-1} and (B) 1600–1000 cm^{-1} . PHBV, poly (3-hydroxybutyrate-co-3-hydroxyvalerate) [Color figure can be viewed at wileyonlinelibrary.com]

2.3.8 | Tensile testing

The tensile properties of aged samples were performed by Zwick/Roell machine according to ISO 527 standard procedure. Young's modulus was measured at a cross-head speed of 1 mm min^{-1} using an incremental clip-on extensometer (Zwick/Roell). The tensile strength and elongation at break were determined at a speed of 50 mm min^{-1} . Five specimens of each dried material were tested.

2.3.9 | Scanning electron microscopy

SEM was performed to examine the fractured surface of samples before and after exposure to hydrothermal aging. The microscopic observations were made in

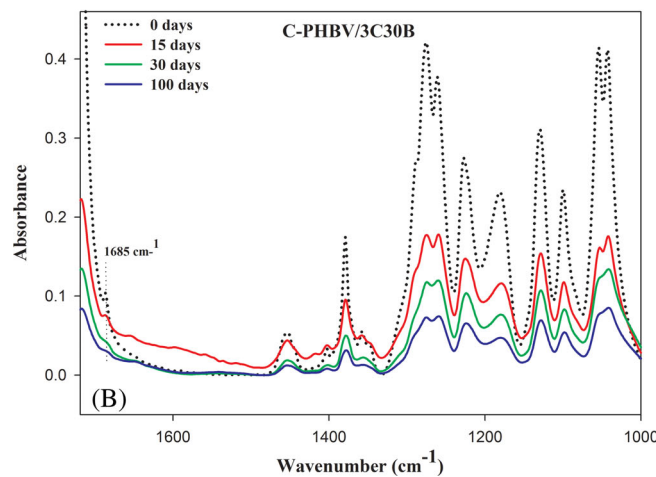
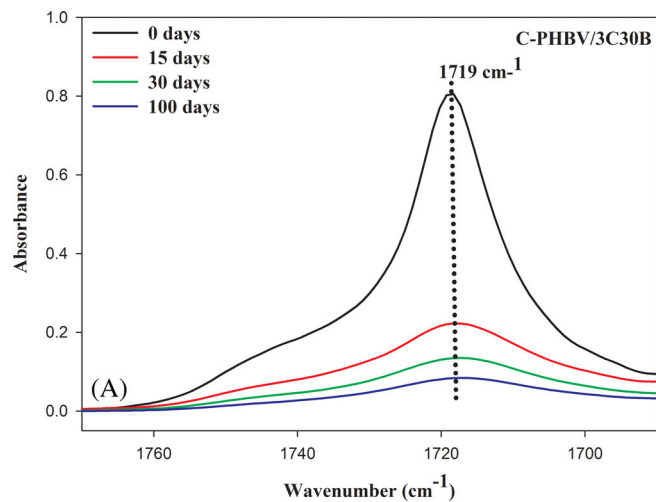


FIGURE 3 FT-IR spectra of C-PHBV/3C30B before and after exposure to hydrothermal aging recorded in the carbonyl region: (A) 1760–1700 cm^{-1} and (B) 1600–1000 cm^{-1} . PHBV, poly (3-hydroxybutyrate-co-3-hydroxyvalerate) [Color figure can be viewed at wileyonlinelibrary.com]

environmental mode using a Quanta 200 FEG (FEI Company) scanning electron microscope. Prior to observations, the fracture surfaces of the films were sputter coated with carbon by evaporator apparatus (Balzers).

3 | RESULTS AND DISCUSSION

3.1 | SEM observations

SEM images of the fractured surface of unexposed and exposed films to hydrothermal aging are illustrated in Figure 1(A)–(D). From Figure 1(A), the SEM micrograph of Cast PHBV before exposure, exhibits a smooth surface in which some black particles in circular form of boron nitride are observed, incorporated as nucleating agent in PHBV matrix. The bionanocomposite sample exhibits the

same surface morphology as the neat polymer (see Figure 1(C)) with however, the presence of some clay tactoids in the PHBV matrix of different size and shape. In previous work [28], Wide angle X-ray diffraction (WAXD) and morphological data by Scanning transmission electron microscopy (STEM) showed that the PHBV/3C30B bionanocomposite exhibits an intercalated structure. After 100 days of exposure to hydrothermal aging, the fracture surface of aged samples shows considerable changes as the appearance of cracks and voids clearly observable in Figure 1(B) and (D).

3.2 | Molecular weight changes

SEC data of unexposed and exposed samples to hydrothermal aging are shown in Table 1. Reduction of about 23% in \bar{M}_w , 7% in \bar{M}_n , and 16% in \bar{D} are observed between neat and Cast PHBV. This is attributed to thermal degradation of matrix polymer during melt processing. From Table 1, after hydrothermal aging, the data show that the values of (\bar{M}_w) and (\bar{M}_n) of both samples are reduced with increasing exposure time. Indeed, after 30 days, there is a decrease in (\bar{M}_w) by roughly 2.5 times for Cast PHBV and 2 times for the PHBV bionanocomposite compared with the unexposed samples. Up to 100 days of exposure, the percent decrease in both (\bar{M}_w) and (\bar{M}_n) is almost 84% and 81% for Cast PHBV and 83 and 75% for C-PHBV/3C30B bionanocomposite, respectively. However, there is no change in the value of polydispersity index (\bar{D}) after exposure. This indicates the prevalence of chains scission mechanism, which is responsible for the materials degradation. Furthermore, the results of solubility test corroborate with those obtained by SEC showing no X-linking formation in the aged samples. Similar result was observed in previous studies [33–34] dealing with accelerated photooxidation and gamma irradiation of PHBV/3C30B bionanocomposite. According to Deroiné et al. [35], chain breakage and ester bond hydrolysis are the main reactions occurring during the degradation of PHAs. It was, however, observed that the average number of chain scissions of C-PHBV/3C30B bionanocomposite is lower than that of Cast PHBV. This phenomenon could be due probably to the addition of C30B in PHBV, which slows down the hydrolytic kinetics of the bionanocomposite sample.

3.3 | Chemical structure changes

Chemical structure changes due to hydrothermal aging of aged samples were evaluated by FT-IR analysis. Representative absorbance spectra in the carbonyl region are

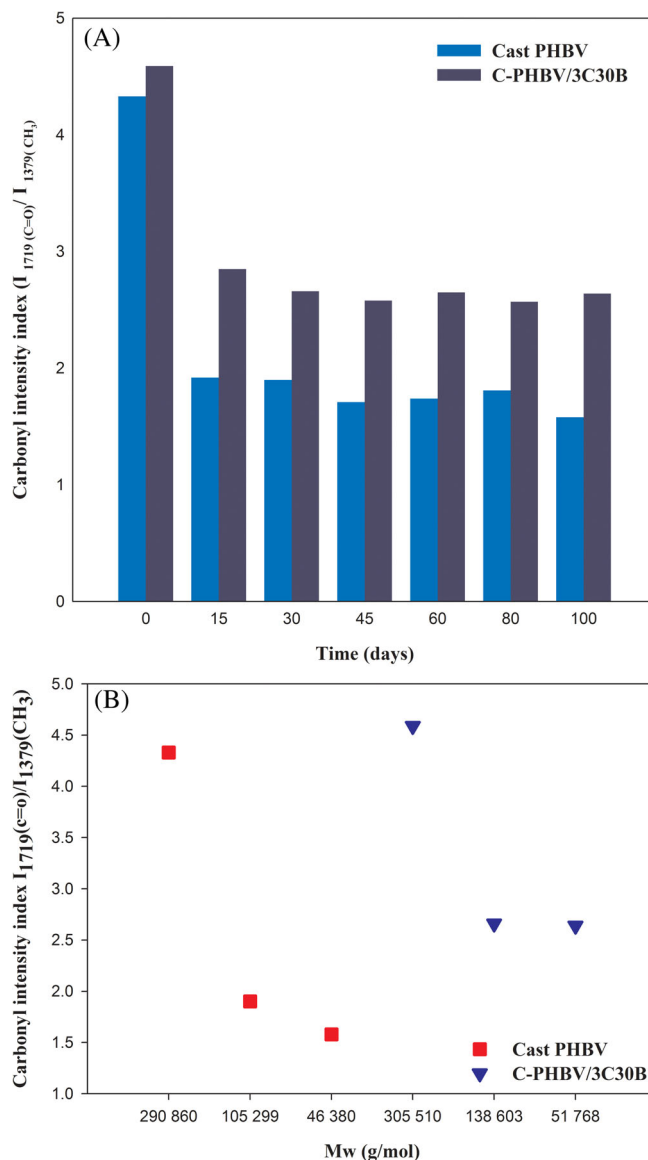


FIGURE 4 Evolution of carbonyl intensity index with exposure time to hydrothermal aging (A) and molecular weight (B) for Cast PHBV and C-PHBV/3C30B. PHBV, poly (3-hydroxybutyrate-co-3-hydroxyvalerate) [Color figure can be viewed at wileyonlinelibrary.com]

shown in Figures 2(A), (B) and 3(A), (B). In Figure 2(A), relative to unexposed Cast PHBV, FT-IR spectra shows a strong band centered at 1719 cm^{-1} , assigned to ester groups. After exposure, the absorption band intensity strongly decreases with exposure time. This results from hydrolysis reactions involving the ester groups of PHBV and hydroxyl groups of moisture leading to changes in chemical structure of aged samples. Similar trend was observed by Badia et al. [25] for PHBV and PHBV/sisal biocomposite under hydrothermal aging. The authors attributed this phenomenon to hydrolytic degradation, resulting in chain scission, which is in a good agreement

FIGURE 5 Evolution of water absorption of Cast PHBV and C-PHBV/3C30B bionanocomposite with exposure time in hygrothermal aging (100% RH, 65°C). PHBV, poly(3-hydroxybutyrate-co-3-hydroxyvalerate) [Color figure can be viewed at wileyonlinelibrary.com]

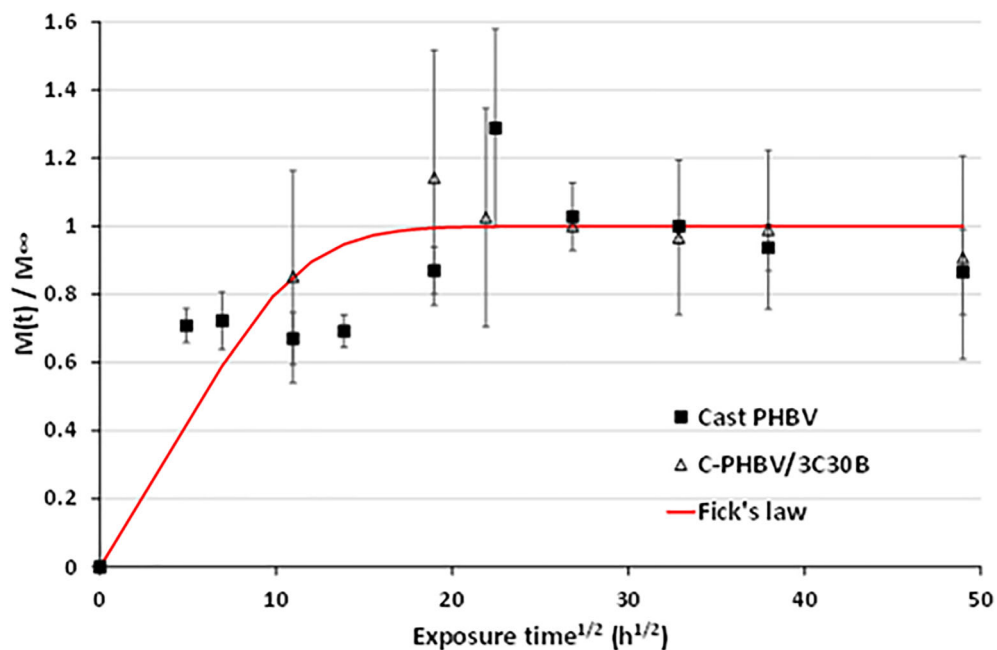


TABLE 2 Evolution of thermal characteristics of neat PHBV, Cast PHBV, and C-PHBV/3C30B bionanocomposite before and after exposure to hygrothermal aging (100% RH, 65°C)

Samples	Exposure time (days)	T_c (°C)	T_{m2} (°C)	T_{m1} (°C)	X_c (%)
Neat PHBV	/	122 ± 0.5	-	172 ± 0.9	69.09 ± 0.5
	0	119 ± 0.5	-	170 ± 0.5	66.10 ± 1
	15	114.5 ± 0.1	-	166 ± 0.2	66.04 ± 0.9
	30	114 ± 0.711	-	165 ± 0.3	66.45 ± 0.7
Cast PHBV	45	3.8 ± 0.2	-	164 ± 0.6	65.68 ± 0.2
	60	113.9 ± 0.8	163 ± 0.1	168 ± 0.1	65.92 ± 0.6
	80	114 ± 0.3	162 ± 0.2	168 ± 0.4	64.46 ± 0.8
	100	113 ± 0.1	161 ± 0.1	167 ± 0.1	64.45 ± 0.2
C-PHBV/3C30B	0	119 ± 0.5	-	165 ± 0.5	63.4 ± 0.5
	15	118.7 ± 0.1	-	163 ± 0.2	64.6 ± 0.1
	30	118.9 ± 0.2	-	164 ± 0.5	58.5 ± 0.2
	45	117.9 ± 0.1	-	162 ± 0.3	62.7 ± 1
	60	117.4 ± 0.4	161 ± 0.2	165 ± 0.2	62.4 ± 0.4
	80	118 ± 0.6	161 ± 1.0	166 ± 1	61.9 ± 0.5
	100	117 ± 0.5	158 ± 0.5	162 ± 0.5	58.4 ± 0.8

Abbreviations: PHBV, poly(3-hydroxybutyrate-co-3-hydroxyvalerate); RH, relative humidity.

with SEC data. Zembouai et al. [36–37] reported also same behavior on the radiolytic degradation of PHBV. In the region of 1600–1000 cm^{-1} , Figure 2(B) shows a significant change in the chemical structure of the aged specimens. Indeed, FT-IR spectra of Cast PHBV show that the absorption band intensity located at $\lambda_{\text{max}} = 1685 \text{ cm}^{-1}$ assigned to C=O groups decreases with exposure time. It is also observed that the band intensity located at $\lambda_{\text{max}} = 1053$ and 1043 cm^{-1} , attributed to C-O groups, are

inversed. The formation of a short absorption band located at $\lambda_{\text{max}} = 1650 \text{ cm}^{-1}$ results from the hydrolysis of ester groups of PHBV leading to formation hydroxyl groups.

The FT-IR spectra of C-PHBV/3C30B bionanocomposite (Figure 3(A), (B)) are almost similar to those of the Cast PHBV. This suggests that the presence of C30B organoclay does not affect the mechanism of hydrolytic degradation of PHBV.

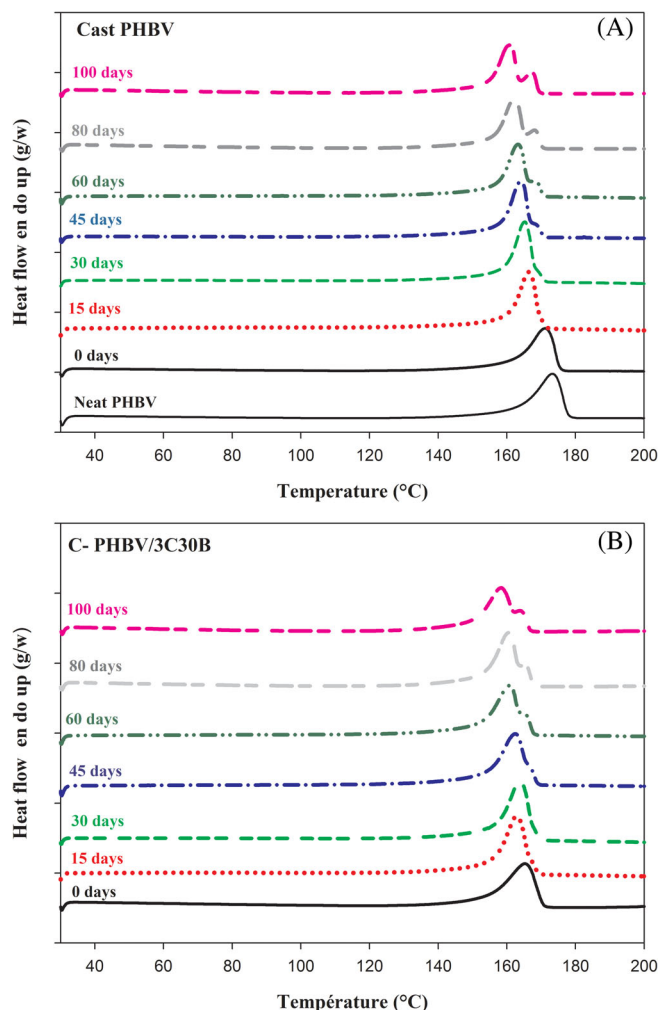


FIGURE 6 DSC thermograms of (A) neat PHBV, Cast PHBV and (B) C-PHBV/3C30B bionanocomposite as a function of exposure time in hygrothermal aging (100% RH, 65°C). PHBV, poly(3-hydroxybutyrate-co-3-hydroxyvalerate) [Color figure can be viewed at wileyonlinelibrary.com]

The determination of the carbonyl intensity index is a usual method to evaluate the level of hydrolytic degradation of polymers. Carbonyl intensity index is defined as the ratio of the absorption band intensity at 1719 cm^{-1} ($\text{C}=\text{O}$)/ 1379 cm^{-1} (CH_3)^[25], which remains unchanged during hygrothermal aging for both Cast PHBV and C-PHBV/3C30B bionanocomposite.

The absorption band at 1379 cm^{-1} which corresponds to the CH_3 asymmetric groups is used as reference and it is useful for normalizing thickness or sample positioning. The results are shown in Figure 4(A). A general decrease of carbonyl intensity index is observed with increasing the exposure time. Furthermore, it is noted that at initial stage of exposure (30 days), both samples already exhibit a rapid decrease in the carbonyl intensity index. Above 45 days of exposure, the carbonyl intensity index is not more affected and remains higher for C-PHBV/3C30B bionanocomposite. This is

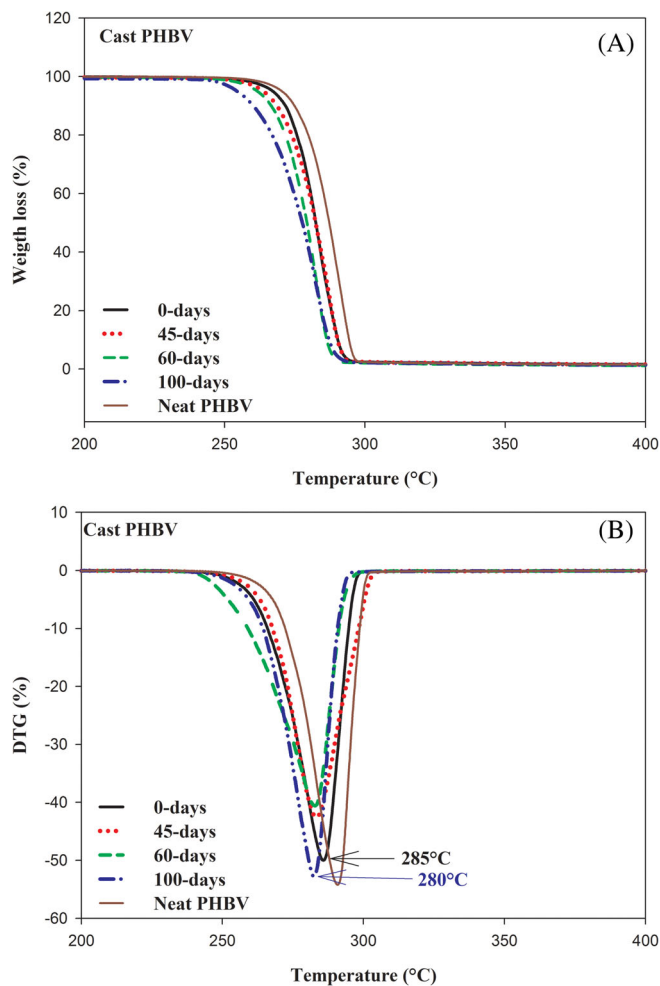


FIGURE 7 (A) TGA and (B) DTG curves of neat PHBV, Cast PHBV before and after exposure to hygrothermal aging (100% RH, 65°C). PHBV, poly(3-hydroxybutyrate-co-3-hydroxyvalerate); TGA, thermogravimetric analysis [Color figure can be viewed at wileyonlinelibrary.com]

consistent with the SEC data. Indeed, the plots in Figure 4(B) display similar trend for both the carbonyl intensity index and molecular weight, that is, the carbonyl intensity index decreases with decreasing the molecular weight.

3.4 | Water absorption

Figure 5 shows the curves of water absorption as a function of exposure time for Cast PHBV and C-PHBV/3C30B bionanocomposite. It is observed that the water absorption plots exhibit similar trend for both samples and a quasi-plateau of roughly 1080 h (45 days) and 720 h (30 days) for Cast PHBV matrix and C-PHBV/3C30B bionanocomposite, respectively. At this stage, the water absorption value (Equation 1) is 0.98% for Cast PHBV and 1.90% for C-PHBV/3C30B. Experimental data show a Fickian's behavior, characterized by a linear relationship

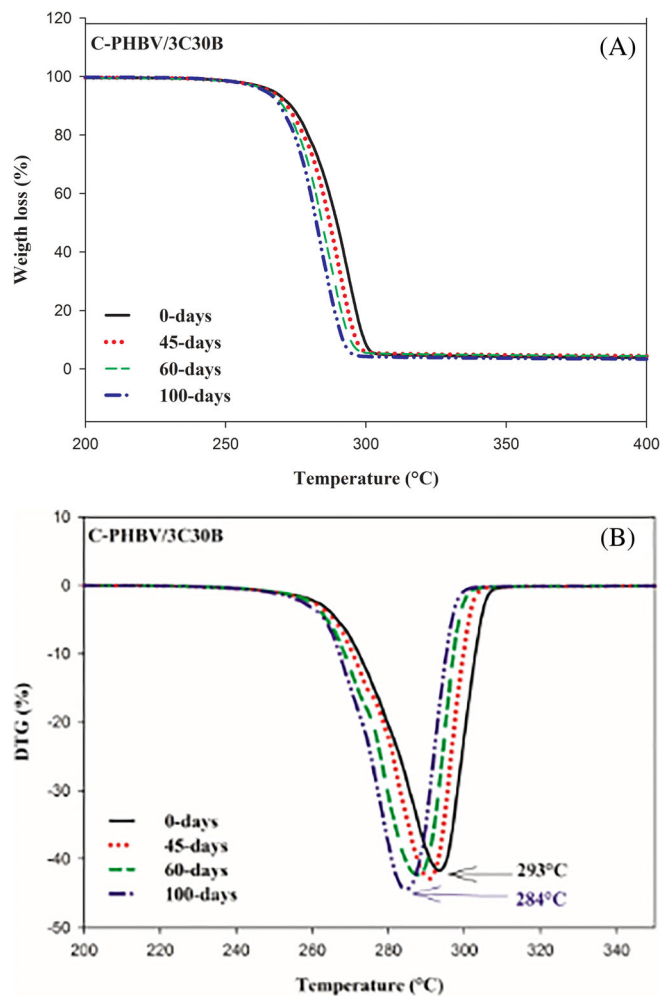


FIGURE 8 Thermograms (A) TGA and (B) DTG of C-PHBV/3C30B bionanocomposite before and after exposure to hygrothermal aging (100% RH, 65°C). PHBV, poly (3-hydroxybutyrate-co-3-hydroxyvalerate); TGA, thermogravimetric analysis [Color figure can be viewed at wileyonlinelibrary.com]

TABLE 3 Decomposition temperature values of neat PHBV, Cast PHBV and C-PHBV/3C30B bionanocomposite before and after exposure to hygrothermal aging (100% RH, 65°C)

Samples	Exposure time (days)	$T_{5\%}$ (°C)	$T_{50\%}$ (°C)	$T_{\max. \text{ rate } T_{\text{mdr}}}$ (°C)	Char (%) at 600 (°C)
Neat PHBV	/	270	287	288	1.2
	0	263	282	285	1.30
Cast PHBV	45	263	282	283	1.35
	60	261	279	282	1.67
	100	254	277	280	1.15
C-PHBV/3C30B	0	266	290	293	3.60
	45	266	288	290	4.04
	60	265	284	287	4.04
	100	264	282	284	3.12

Abbreviations: PHBV, poly(3-hydroxybutyrate-co-3-hydroxyvalerate); RH, relative humidity.

between water absorption and square root of time in the first few days of hygrothermal aging, followed by saturation for both samples. This trend has already been reported for PHBV and polylactide (PLA) [26,35,38–40]. The water diffusion coefficients (D) at 65°C, obtained from the best fit of experimental data according to Equation (2), are similar and their values are estimated to 9.0×10^{-7} and $9.3 \times 10^{-7} \text{ cm}^2 \text{ h}^{-1}$ for Cast PHBV and C-PHBV/3C30B bionanocomposite, respectively. The literature [38,41–42] reported that the capacity of water absorption and its rate of diffusion in nanocomposites depending on various factors such as: specific surface area of the clay, micro void existing in the polymer/clays interfaces, free volume in polymer matrix, the tortuosity of water diffusion into the polymeric matrix, molecular relaxation and polymer matrix crystallinity. The higher amount of water absorption in the PHBV bionanocomposite is related to the hydrophilic nature of organoclays (C30B). Due to their polar hydroxyl groups (OH), C30B may interact with the water molecules through hydrogen bonds resulting in the enhancement of wettability of PHBV. It should be also pointed out that beyond 60 days of exposure, the sample weight of both materials decreases, due to hydrolysis reactions as revealed by SEC and FT-IR analyses, and probable consecutive leaching of the samples.

3.5 | Thermal properties changes

Table 2 summarizes the values of the main thermal characteristics of neat PHBV, Cast PHBV and C-PHBV/3C30B bionanocomposite before and during the hygrothermal aging. Moreover, Figure 6 shows the DSC thermograms

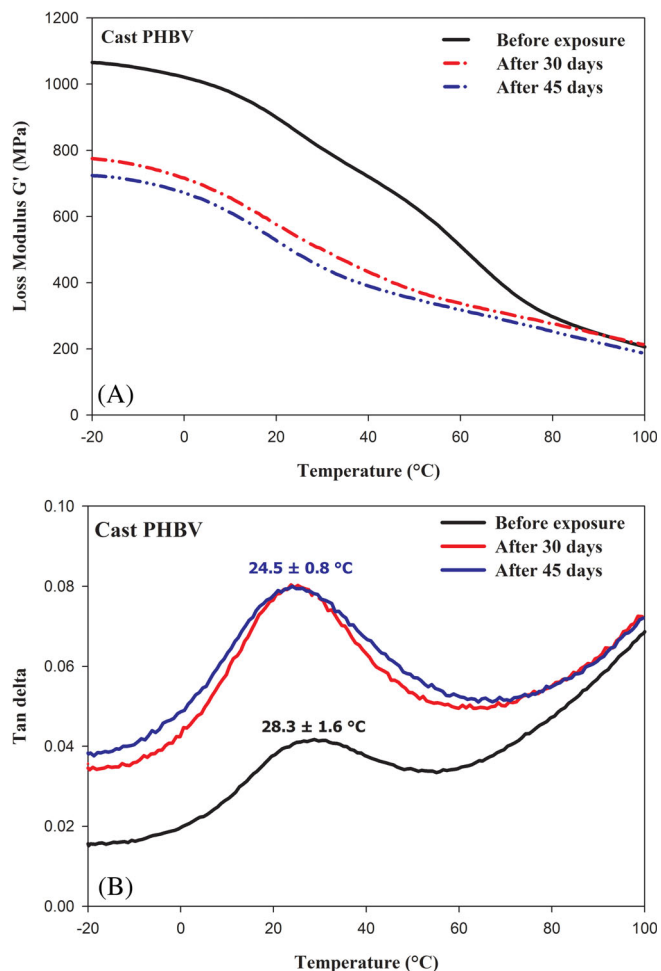


FIGURE 9 Evolution of (A) storage modulus (G') and (B) loss factor ($\tan \delta$) for Cast PHBV at various exposure times to hygrothermal aging (100% RH, 65°C). PHBV, poly(3-hydroxybutyrate-co-3-hydroxyvalerate); [Color figure can be viewed at wileyonlinelibrary.com]

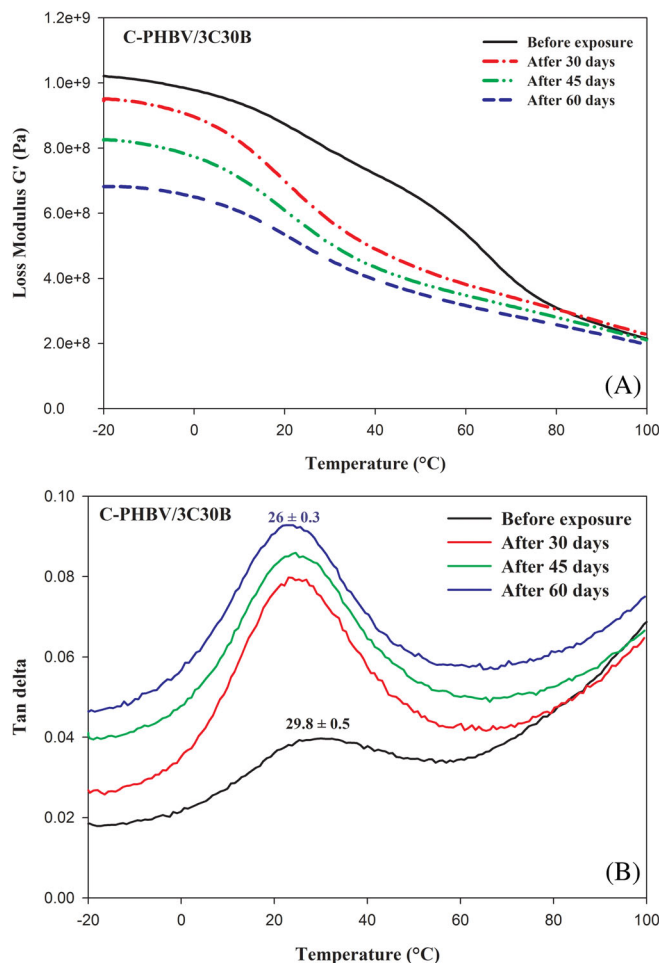


FIGURE 10 Evolution of (A) storage modulus (G') and (B) loss factor ($\tan \delta$) for C-PHBV/3C30B nanocomposite at various exposure times to hygrothermal aging (100% RH, 65°C). PHBV, poly(3-hydroxybutyrate-co-3-hydroxyvalerate); [Color figure can be viewed at wileyonlinelibrary.com]

recorded during the second heating scans for aged samples at various exposure times.

Table 2 indicates a decrease in melting temperature (T_m) by a few degrees for Cast PHBV and C-PHBV/3C30B bionanocomposite with increasing exposure time. Furthermore, over 45 days, DSC thermograms in Figure 6 clearly show the appearance of double melting peaks for both samples, that is, the primary melting peak (T_{m1}) and a secondary melting peak (T_{m2}) that becomes predominant and appears at lower temperature. The literature^[43–44] reported that the double melting peak in biopolyesters may result from recrystallization process. The overall decrease in T_m is ascribed to the formation of short chain segments with lower molecular weight due to chain scission through hydrolysis, and the consecutive formation of imperfect crystals. Thus, the lower melting peaks correspond to imperfect crystallites formed after melting and recrystallization of

aged samples, while the higher melting peaks correspond to more perfect crystals that melt at higher temperature^[42,45]. Table 2 also shows a slight decrease of T_c and X_c with increasing exposure time. Indeed after 100 days of exposure, T_c decreases by almost 6 and 2°C, and X_c decreases by almost 2% and 5% for Cast PHBV and C-PHBV/3C30B bionanocomposite, respectively. The decrease of T_c after aging can be related to reorganization of shorter macromolecular fragments in an order structure at lower temperatures. Whereas, the decrease of X_c results from the diffusion of water that restricts the recrystallization. Further, the large interfacial developed between the molecules of water and OMMT should reduce the mobility of the polymer chains^[21,46]. On the other hand, a decrease in T_c , T_m , and X_c is observed between the neat and Cast PHBV, that should be the result of PHBV degradation during melt processing as shown in SEC experiments.

TABLE 4 Tensile properties changes of Cast PHBV and C-PHBV/C30B bionanocomposite before and after exposure to hygrothermal aging (100% RH, 65°C)

Samples	Exposure time (h)	Young's modulus (MPa)	Tensile strength (MPa)	Elongation at break (%)
Cast PHBV	0	1020 ± 51	27.0 ± 1.4	2.9 ± 0.2
	15	1070 ± 61	25.7 ± 0.2	3.0 ± 0.3
	30	741 ± 58	15.4 ± 1.9	2.6 ± 0.4
	45	681 ± 73	11.4 ± 1.2	2.0 ± 0.4
	60	657 ± 56	6.2 ± 2.4	1.4 ± 0.8
C-PHBV/3C30B	0	1180 ± 42	28.0 ± 1.3	2.9 ± 0.1
	15	1160 ± 42	31.7 ± 3.0	3.2 ± 0.2
	30	848 ± 75	24.7 ± 2.0	3.2 ± 0.3
	45	818 ± 88	19.3 ± 4.0	2.5 ± 0.6
	60	882 ± 79	14.7 ± 2.4	2.8 ± 0.5

Abbreviations: PHBV, poly(3-hydroxybutyrate-co-3-hydroxyvalerate); RH, relative humidity.

3.6 | Thermal stability

TGA and DTG thermograms for neat PHBV, Cast PHBV, and C-PHBV/3C30B bionanocomposites as function of exposure time are shown in Figures 7(A), (B) and 8(A), (B), respectively. The values of degradation temperatures are presented in Table 3.

Before hygrothermal aging, Cast PHBV exhibits one-step decomposition with a weight loss between 260 and 290°C. The DTG curves also display a minimum at roughly 285°C associated with the temperature at maximum degradation rate, as shown in Figure 7(B). The results indicate also that the thermal stability of neat PHBV is reduced after processing due to the decrease in the molar mass as shown by SEC data.

The bionanocomposite C-PHBV/3C30B also shows a one-step decomposition with a temperature at maximum degradation rate at around 293°C (Figure 8(B)), hence higher than non-aged Cast PHBV. The enhancement of thermal stability with addition of organoclay C30B in PHBV is attributed to the tortuosity phenomena which restricts the diffusion of oxygen, thus reducing the rate of decomposition [47]. After hygrothermal exposure, the decomposition temperatures for both samples decrease with increasing the exposure time.

Table 3 shows that after 100 days, $T_{5\%}$ and $T_{m_{dr}}$ decrease by 9 and 5°C for Cast PHBV, respectively. For the bionanocomposite material, $T_{5\%}$ and $T_{m_{dr}}$ also shifted to lower values with a decrease by 2 and 9°C, respectively. The decrease of thermal stability may be due to the effects of both thermal and hydrolytic degradation. It should be pointed out that the bionanocomposite exhibited the better thermal stability compared to neat PHBV even at 100 days of aging.

3.7 | Viscoelastic properties changes

Dynamic mechanical measurements were performed to examine the effect of hygrothermal aging on the viscoelastic properties of Cast PHBV and PHBV/C30B bionanocomposite samples. Figures 9(A), (B) and 10 (A), (B) show the evolution of storage modulus (G') and loss factor ($\tan \delta$) with exposure time for aged samples, respectively. Before exposure to hygrothermal aging, it is noticed that the storage modulus (G') of the bionanocomposite is higher than that of Cast PHBV. Indeed at 20°C, the value of G' is roughly 896 and 1021 MPa for Cast PHBV and C-PHBV/3C30B bionanocomposite, respectively. It is also observed that $\tan \delta$ shifts toward a higher temperature for the bionanocomposite. $\tan \delta$ of Cast PHBV is located almost at $28.3 \pm 1.6^\circ\text{C}$ which increases very slightly to $29.8 \pm 0.5^\circ\text{C}$ for C-PHBV/3C30B bionanocomposite. The improvement of G' and to a less extent of α -transition temperature is due to a good dispersion of C30B and also to its interactions with the polymer matrix restricting the macromolecular chains mobility. After exposure to hygrothermal aging, the storage modulus is significantly reduced for both aged samples with time. In addition, C-PHBV/3C30B bionanocomposite is less affected by hydrothermal aging compared with Cast PHBV; Indeed, after 45 days of exposure at 20°C, G' of Cast PHBV decreases by almost 42% with respect to that of unexposed sample, whereas for the bionanocomposite, G' is reduced by about 23% after 60 days. Above 45 and 60 days of aging, Cast PHBV and C-PHBV/3C30B were very brittle to be tested. From Figures 9(B) and 10(B), it can be seen that the shape of $\tan \delta$ signals indicates a shift in the α -transition temperature toward lower temperatures

for both samples as well as a significant increase in Tan δ magnitude. Indeed, after 60 days of exposure, the Cast PHBV and bionanocomposite exhibit an α -transition at 28.3 ± 1.6 and $29.8 \pm 0.5^\circ\text{C}$, which slightly decreases to 24.5 ± 0.8 and $26.0 \pm 0.3^\circ\text{C}$, respectively. This increased damping and earlier activated molecular motion of the aged samples, revealed by the higher Tan δ and lower α -transition temperature respectively, is due likely to the decrease in the molar mass resulting from the hydrolytic degradation of PHBV.

3.8 | Tensile properties changes

The results of tensile properties of aged samples are summarized in Table 4. It is observed that Young's modulus, tensile strength, and elongation at break for Cast PHBV are reduced along hygrothermal aging.

After 60 days of exposure, the values for Young's modulus, tensile strength and elongation at break are decreased by 36%, 77%, and 52%, respectively, as compared to nonaged PHBV. In addition, the samples are too brittle and cannot be tested. According to the literature [33–34], the decrease in Young's modulus and strength of PHBV during aging is attributed to the decrease of molar mass. Furthermore, the mechanical properties of the bionanocomposite are less altered compared with Cast PHBV. Indeed, Young's modulus, tensile strength and elongation at break were reduced by 25%, 47%, and 5%, respectively. Accordingly, the incorporation of C30B in PHBV counterbalances the detrimental effects of aging on the tensile properties of the PHBV bionanocomposite.

4 | CONCLUSION

The effect of hygrothermal aging at 65°C and 100% RH on neat PHBV and its bionanocomposite C-PHBV/C30B was investigated up to 100 days. It can be concluded that the incorporation of C30B into PHBV matrix increased the water absorption. The aged materials exhibited a strong modification on the chemical structure. Indeed, the carbonyl intensity index decreased during degradation, attesting for a hydrolysis phenomenon upon aging. However, the extent of decrease in the carbonyl intensity index was lower for the C-PHBV/3C30B bionanocomposite. Hydrolysis process via chain scission mechanism leads to a decrease in the molecular mass of both Cast PHBV and bionanocomposite, being however, less pronounced for the latter. Melting and crystallization temperature as well as the degree of crystallinity decreased with increasing exposure times. Thermal

stability of aged Cast PHBV and aged C-PHBV/3C30B were reduced but remained higher for the bionanocomposite. Tensile and viscoelastic properties of PHBV were significantly affected by aging, whereas these properties were more stable for the bionanocomposite. The study revealed that the dispersion of C30B in PHBV allows to improve its hygrothermal stability and better maintained its physical and mechanical properties up to 60 days. These findings can be of interest for applications where functional properties of PHBV should be retained for a while in hygrothermal conditions at 65°C and 100% RH.

ACKNOWLEDGMENTS

The study was supported by Erasmus Mundus European program (Averroes 4). The technical assistance in the SEC analysis by Jean Coudane and Sylvie Hunger are gratefully acknowledged.

ORCID

Kahina Iggui  <https://orcid.org/0000-0001-8353-8292>

Mustapha Kaci  <https://orcid.org/0000-0002-4283-9803>

Nicolas Le Moigne  <https://orcid.org/0000-0002-1218-7090>

Anne Bergeret  <https://orcid.org/0000-0001-7118-6584>

REFERENCES

- [1] A. L. Rivera-Briso, Á. Serrano-Aroca, *Polymers (Basel)* **2018**, 10, 732.
- [2] Z. Li, J. Yang, X. J. Loh, *NPG Asia Mater* **2016**, 8, 265.
- [3] Y. Li, T. J. Strathmann, *Green Chem* **2019**, 21, 5586.
- [4] E. Bugnicourt, P. Cinelli, A. Lazzeri, V. Alvarez, *Express Polym Lett* **2014**, 8, 791.
- [5] H. Liu, Z. Gao, X. Hu, Z. Wang, T. Su, L. Yang, S. Yan, *J Polym Environ* **2017**, 25, 156.
- [6] F. Massod, M. Aziz, H. Haider, *Int Biodeterior Biodegradation* **2018**, 126, 1.
- [7] Y. Phua, W. S. Chow, I. Mohd, *J Thermoplast Compos Mater* **2010**, 14, 133.
- [8] L. Zaidi, S. Bruzaud, A. Bourmaud, P. Médéric, M. Kaci, *J Appl Polym Sci* **2010**, 116, 1357.
- [9] J. K. Pandey, K. Raghunatha Reddy, A. Pratheep Kumar, R. P. Singh, *Polym Degrad Stab* **2005**, 88, 234.
- [10] S. Slater, D. Glassner, E. Vink, T. Gerngross, in *Biopolym Online*, Vol. 10 (Ed: A. Steinbüchel) **2006**, p. 474.
- [11] V. M. Correlo, E. D. Pinhp, I. Pashkuleva, M. Bhattacharya, N. M. Neves, R. L. Reis, *Macromol Biosci* **2007**, 7, 354.
- [12] W. S. Chow, A. Abu Bakar, Z. A. Mohd Ishak, *J Appl Polym Sci* **2005**, 98, 780.
- [13] H. Chen, F. Chen-Xia, W. B. Zhang, J. H. Yang, T. Huang, N. Zhang, Y. Wang, *Polym Degrad Stab* **2013**, 98, 198.
- [14] H. M. Chen, Y. P. Wang, J. Chen, J. H. yang, N. Zhang, T. Huang, *Polym Degrad Stab* **2013**, 98, 2672.
- [15] Z. A. Mohd Ishak, J. P. Berry, *J Appl Polym Sci* **1994**, 51, 2145.
- [16] G. Gorrasi, R. Pantani, *Polym Degrad Stab* **2013**, 98, 1006.

- [17] A. V. Janorkar, A. T. Metters, D. E. Hirt, *Macromolecules* **2004**, 37(24), 9151.
- [18] O. Gil-Castell, J. D. Badia, T. Kittikorn, E. Stromberg, A. Martinez-Felipa, M. EK, S. Karlsson, A. Ribes-Greus, *Polym Degrad Stab* **2014**, 108, 212.
- [19] J. D. Badia, I. Santonja-blasco, A. Martinez-Felipe, A. Ribes-Greus, *Polym Degrad Stab* **2012**, 97, 1881.
- [20] T. G. Volova, A. N. Boyandin, A. D. Vaselliv, V. A. Karpov, S. V. Prundmkova, O. V. Mishukova, *Polym Degrad Stab* **2010**, 95, 2350.
- [21] Y. Phua, W. S. Chow, Z. A. Mohd Ishak, *Polym Degrad Stab* **2011**, 96, 1194.
- [22] V. A. Zhuikov, Y. V. Zhuikova, T. K. Makhina, V. L. Myshkina, A. Rusakov, A. Useinov, V. V. Voinova, G. A. Bonartseva, A. A. Berlin, A. P. Bonartsev, A. L. Iordanskii, *Polymers* **2020**, 12, 728.
- [23] K. Mazur, S. Kuciel, *Molecules* **2019**, 24, 3538.
- [24] V. A. D. Marinho, L. H. Carvalho, E. L. Canedo, *Am Instit Phys* **2015**. 1664, 060003. <https://doi.org/10.1063/1.4918421>.
- [25] J. D. Badia, T. Kittikorn, E. Strömberg, L. Santonja-Blasco, A. Martínez-Felipe, A. Ribes-Greus, M. Ek, S. Karlsson, *Polym Degrad Stab* **2014**, 108, 166.
- [26] H. Ventura, J. Claramunt, M. A. Rodríguez- Pérez, M. Ardanuy, *Polym Degrad Stab* **2017**, 142, 129.
- [27] R. N. Silva, L. R. C. Silva, A. C. L. Morais, T. S. Barbosa, *J Thermoplast Compo Mater* **2019**, 89270571985604. <https://doi.org/10.1177/0892705719856044>.
- [28] K. Iggui, N. Le Moigne, S. Cambe, J. R. Degorce-Dumas, M. Kaci, A. Bergeret, *Polym Degrad Stab* **2015**, 119, 77.
- [29] V. Berthé, L. Ferry, J. C. Bénézet, A. Bergeret, *Polym Degrad Stab* **2010**, 95, 262.
- [30] J. Crank, *The mathematics of Diffusion*, 2nd ed., Clarendon Press, Oxford **1975**.
- [31] F. Rosario, E. Corradini, S. A. Casarin, J. A. M. Agnelli, *J Polym Environ* **2013**, 21, 789.
- [32] P. J. Barham, A. Keller, E. L. Otun, P. A. Holmes, *J Mater Sci* **1984**, 19, 2781.
- [33] K. Iggui, M. Kaci, M. Mahlous, N. Le Moigne, A. Bergeret, *J Renew Mater* **2019**, 7, 807.
- [34] K. Iggui, M. Kaci, N. Le Moigne, A. Bergeret, *J Renew Mater* **2018**, 6, 288.
- [35] M. Deroiné, A. Le Duigou, Y. M. Corre, P. Y. Le Gac, P. Davies, G. César, S. Bruzaud, *Polym Degrad Stab* **2014**, 105, 237.
- [36] I. Zembouai, M. Kaci, S. Bruzaud, L. Dumazert, A. Bourmaud, *Polym Test* **2016**, 49, 29.
- [37] I. Zembouai, M. Kaci, S. Bruzaud, I. Pillin, J. L. Audic, *Polym Degrad Stab* **2016**, 132, 117.
- [38] C. Y. Tang, D. Z. Chen, T. M. Yue, K. C. Chan, C. P. Tsui, P. H. F. Yu, *Compos Sci Technol* **2008**, 68, 1927.
- [39] A. Le Duigou, P. Davies, C. Baley, *Polym Degrad Stab* **2009**, 94, 1151.
- [40] M. Deroiné, A. Le Duigou, Y. M. Corre, P. Y. Le Gac, P. Davies, G. César, S. Bruzaud, *Polym Degrad Stab* **2014**, 108, 319.
- [41] B. Harintharavimal, H. Azman, I. Muhammad, W. Mat Uzir, *J Polym Environ* **2011**, 19, 863.
- [42] T. Aouat, M. Kaci, J. M. Lopez-Cuesta, E. Devaux, *Front Mater* **2019**, 6, 323.
- [43] L. Santonja-Blasco, A. Ribes-Greus, R. G. Alamo, *Polym Degrad Stab* **2013**, 98, 771.
- [44] Y. Shieh, G. Liu, *J Polym Sci Part B Polym Phys* **2007**, 45, 466.
- [45] M. Ma, W. Zhou, *Ind Eng Chem Res* **2015**, 54, 2599.
- [46] S. S. Ray, M. Bousmina, K. Okamoto, *Macromol Mater Eng* **2005**, 290, 759.
- [47] L. Zaidi, M. Kaci, S. Bruzaud, A. Bourmaud, Y. Grohens, *Polym Degrad Stab* **2010**, 95, 1751.